Eidgenössische Technische Hochschule Zürich

Ecole polytechnique fédérale de Zurich
Politecnico federale di Zurigo
Swiss Federal Institute of Technology Zurich

Stable finite difference schemes for the magnetic induction equation with Hall effect

P. Corti and S. Mishra

Research Report No. 2011-23
April 2011

Seminar für Angewandte Mathematik
Eidgenössische Technische Hochschule
CH-8092 Zürich
Switzerland

STABLE FINITE DIFFERENCE SCHEMES FOR THE MAGNETIC INDUCTION EQUATION WITH HALL EFFECT

PAOLO CORTI AND SIDDHARTHA MISHRA

Abstract. We consider a sub-model of the Hall-MHD equations: the so-called magnetic induction equations with Hall effect. These equations are non-linear and include third-order spatial and mixed derivatives. We show that the energy of the solutions is bounded and design finite difference schemes that preserve the energy bounds for the continuous problem. We design both divergence preserving schemes and schemes with bounded divergence. The schemes are compared on a set of numerical experiments that demonstrate the robustness of the proposed schemes.

1. Introduction

Plasmas are increasingly becoming important in a variety of fields like astrophysics, solar physics, electrical and aerospace engineering. Specific problems include the study of supernovas, accretion disks, waves in the solar atmosphere, magnetic confinement fusion, the design of plasma thrusters for spacecraft propulsion and of circuit breakers in the electrical power industry. It is standard to model plasmas as magnetized fluids with fluid motion shaping and in turn being shaped by magnetic fields. The base model for such interaction are the equations of Magneto-Hydro Dynamics (MHD):

$$\frac{\partial \rho}{\partial t} = -\nabla \cdot (\rho \mathbf{u}), \tag{1.1}$$

$$\frac{\partial (\rho \mathbf{u})}{\partial t} = -\nabla \left\{ \rho \mathbf{u} \otimes \mathbf{u} + \left(p + \frac{|\mathbf{B}|^2}{2} \right) \mathbf{I}_{3\times 3} - \mathbf{B} \otimes \mathbf{B} \right\}, \tag{1.2}$$

$$\frac{\partial \mathcal{E}}{\partial t} = -\nabla \left\{ \left(\mathcal{E} + p - \frac{|\mathbf{B}|^2}{2} \right) \mathbf{u} + \mathbf{E} \times \mathbf{B} \right\}, \tag{1.3}$$

$$\frac{d \mathbf{B}}{dt} = -\nabla \times \mathbf{E}. \tag{1.4}$$

Here ρ, $\mathbf{u}$, p are the gas density, velocity and pressure respectively. $\mathbf{E}$ and $\mathbf{B}$ are the electric and magnetic fields. The total energy $\mathcal{E}$ is given by the equation of state:

$$\mathcal{E} = \frac{p}{\gamma - 1} + \frac{\rho |\mathbf{u}|^2}{2} + \frac{|\mathbf{B}|^2}{2}. \tag{1.5}$$

Here, γ is the gas constant. Equations from (1.1) to (1.3) represent the conservation of mass, momentum and energy and (1.4) describes the Maxwell's equations for the evolution of the magnetic field.

In addition, the absence of magnetic monopoles implies that the MHD equations have to obey the divergence constraint:

$$\nabla \cdot \mathbf{B} = 0. \tag{1.6}$$

We need to describe the electric field in (1.4) to complete the MHD equations. Different choices for the electric field (Ohm's law) lead to different MHD models. The most popular MHD model is the ideal MHD equation where the electric field is given by

$$\mathbf{E} = -\mathbf{u} \times \mathbf{B}. \tag{1.7}$$

Date: April 28, 2011.

The ideal MHD equations are extremely successful in several applications, see [1] for an overview and [3] for a recent application in solar physics. However a major limitation of the ideal MHD equations is the requirement that the magnetic field lines are frozen into the fluid. In many interesting applications in both astrophysics and engineering, we observe magnetic reconnection i.e. the magnetic topology changes during the flow [7]. In order to induce reconnection, a possible mechanism is magnetic resistivity resulting in the Ohm's law:

$$\mathbf{E} = -\mathbf{u} \times \mathbf{B} + \eta \mathbf{J}. \tag{1.8}$$

Here $\mathbf{J}$ is the current density and η is the resistivity parameter. The resulting equations are termed the *resistive* MHD equations. However, the resistive MHD equations do not suffice in modeling *fast magnetic reconnection*.

A more effective alternative is to include the Hall effect [7, 10]. The resulting Ohm's law is

$$\mathbf{E} = -\mathbf{u} \times \mathbf{B} + \eta \mathbf{J} + \frac{\delta_i}{L_0} \frac{\mathbf{J} \times \mathbf{B}}{\rho} + \left(\frac{\delta_e}{L_0} \right)^2 \frac{1}{\rho}. \left[\frac{d\,\mathbf{J}}{dt} + (\mathbf{u} \cdot \nabla)\, \mathbf{J} \right]. \tag{1.9}$$

Here L_0 is the normalizing length unit, and δ_e and δ_i denote electron and ion inertia respectively; they are related to electron-ion mass ratio by $(\frac{\delta_e}{\delta_i})^2 = \frac{m_e}{m_i}$. The term $\mathbf{J} \times \mathbf{B}$ is the so-called Hall term and $\mathbf{J}_t + (\mathbf{u} \cdot \nabla)\mathbf{J}$ is the electron inertia term [7].

The equations need to be completed by specifying Ampére's law for the current:

$$\mathbf{J} = \nabla \times \mathbf{B}. \tag{1.10}$$

The MHD equations together with Ohm's law (1.9) and the above Ampére's law are termed as the Hall MHD equations. The Hall MHD equations are non-linear, high-order equations and are extremely complicated to study in a mathematically rigorous manner. There have been various numerical studies of the Hall MHD equations in [13, 10] and references therein. However, all these papers tackle the problem from a computational point of view and do not include any rigorous results.

In contrast to the above papers where schemes were designed for the full Hall MHD equations, we adopt a different approach. First, we consider a sub-model: the Hall induction equations,

$$\begin{aligned} \frac{\partial}{\partial t} \left[\mathbf{B} + \left(\frac{\delta_e}{L_0} \right)^2 \frac{1}{\rho} \nabla \times (\nabla \times \mathbf{B}) \right] &= \nabla \times (\mathbf{u} \times \mathbf{B}) - \eta \nabla \times (\nabla \times \mathbf{B}) \\ &- \left(\frac{\delta_e}{L_0} \right)^2 \frac{1}{\rho} \nabla \times ((\mathbf{u} \cdot \nabla)(\nabla \times \mathbf{B})) - \frac{\delta_i}{L_0} \frac{1}{\rho} \nabla \times ((\nabla \times \mathbf{B}) \times \mathbf{B}). \end{aligned} \tag{1.11}$$

The Hall induction equations are augmented with the divergence constraint (1.6). Here, the unknowns are the magnetic field $\mathbf{B}$ and the velocity field $\mathbf{u}$ is specified a priori. The parameters are as before. Observe that the Hall induction equations are still non-linear with the non-linearity being present in the Hall term. Furthermore, the equations contain second-order spatial derivatives (resistivity) and third-order spatial and spatio-temporal derivatives (electron inertia).

In this paper, we investigate the Hall induction equations from a mathematical point of view and derive stability estimates. The key tool will be to symmetrize the advection terms in (1.11) using the divergence constraint. See [2, 6, 5, 8] for the use of this technique for the ideal magnetic induction equations and the resistive induction equations. We then derive energy estimates in the Sobolev space H^1 for the Hall induction equations with smooth velocity fields.

We also derive stable finite difference schemes for the Hall induction equations (1.11) in this paper. These schemes preserve a discrete version of the energy estimate. In particular, we discuss both divergence preserving schemes and schemes that are based on the symmetric form of the equation and may not preserve a discrete version of the divergence constraint. Numerical experiments demonstrating the robust performance of the proposed schemes are presented. To the best of our knowledge, the proposed schemes are the first set of (rigorously proven) stable schemes for the Hall induction equations.

The rest of the paper is organized as follows: in section 2, we study the continuous problem for the Hall induction equations and show energy estimates. Stable numerical schemes that satisfy a discrete version of the energy inequality are presented in section 3 and we present numerical experiments in section 4.

2. The Continuous Problem

The main aim of this section is to derive energy estimates for the continuous problem corresponding to the Hall induction equations (1.11). It turns out that the advection terms in (1.11) are not symmetric and impair the derivation of an energy estimate. We will symmetrize this term (see [2, 6, 5]) by using a the vector identity

$$\nabla \times (\mathbf{u} \times \mathbf{B}) = (\mathbf{B} \cdot \nabla)\mathbf{u} - \mathbf{B}(\nabla \cdot \mathbf{u}) + \mathbf{u}(\nabla \cdot \mathbf{B}) - (\mathbf{u} \cdot \nabla)\mathbf{B}. \tag{2.1}$$

We use the divergence constraint (1.6) and subtract $\mathbf{u}(\nabla \cdot \mathbf{B})$ from (1.11) to obtain the symmetric form of the Hall induction equations:

$$\begin{aligned}\frac{\partial}{\partial t}\left[\mathbf{B} + \left(\frac{\delta_e}{L_0}\right)^2 \frac{1}{\rho}\,\nabla \times (\nabla \times \mathbf{B})\right] &= (\mathbf{B} \cdot \nabla)\mathbf{u} - \mathbf{B}(\nabla \cdot \mathbf{u}) - (\mathbf{u} \cdot \nabla)\mathbf{B} - \eta \nabla \times (\nabla \times \mathbf{B}) \\ &- \left(\frac{\delta_e}{L_0}\right)^2 \frac{1}{\rho}\nabla \times ((\mathbf{u} \cdot \nabla)(\nabla \times \mathbf{B})) - \frac{\delta_i}{L_0}\frac{1}{\rho}\nabla \times ((\nabla \times \mathbf{B}) \times \mathbf{B})\,.\end{aligned} \tag{2.2}$$

We show the following energy estimate for the symmetric form of the Hall induction equations,

Theorem 2.1. *Let the velocity field $\mathbf{u} \in C^2(\mathbb{R}^3)$. Furthermore, assume that the solution $\mathbf{B}$ of (2.2) decays to zero at infinity, then following apriori estimate holds:*

$$\begin{aligned}&\frac{d}{dt}\left(\|\mathbf{B}\|^2_{L^2(\mathbb{R}^3)} + \left(\frac{\delta_e}{L_0}\right)^2 \frac{1}{\rho}\|\nabla \times \mathbf{B}\|^2_{L^2(\mathbb{R}^3)}\right) \\ &\leq C\left(\|\mathbf{B}\|^2_{L^2(\mathbb{R}^3)} + \left(\frac{\delta_e}{L_0}\right)^2 \frac{1}{\rho}\|\nabla \times \mathbf{B}\|^2_{L^2(\mathbb{R}^3)}\right)\end{aligned} \tag{2.3}$$

with C being a constant that depend on $\mathbf{u}$ and its derivatives only.

Proof. To simplify the notation and emphasize the symmetry of the equation, we rewrite the term $(\mathbf{B} \cdot \nabla)\mathbf{u}$ in the matrix form obtaining:

$$\begin{aligned}\frac{\partial \mathbf{B}}{\partial t} + \left(\frac{\delta_e}{L_0}\right)^2 \frac{1}{\rho}\nabla \times (\nabla \times \frac{\partial \mathbf{B}}{\partial t}) &= C\mathbf{B} - (\nabla \cdot \mathbf{u})\mathbf{B} - (\mathbf{u} \cdot \nabla)\mathbf{B} - \eta \nabla \times (\nabla \times \mathbf{B}) \\ &- \left(\frac{\delta_e}{L_0}\right)^2 \frac{1}{\rho}\nabla \times ((\mathbf{u} \cdot \nabla)(\nabla \times \mathbf{B})) - \frac{\delta_i}{L_0}\frac{1}{\rho}\nabla \times ((\nabla \times \mathbf{B}) \times \mathbf{B})\end{aligned}$$

where

$$C = \begin{pmatrix} \partial_x u^1 & \partial_y u^1 & \partial_z u^1 \\ \partial_x u^2 & \partial_y u^2 & \partial_z u^2 \\ \partial_x u^3 & \partial_y u^3 & \partial_z u^3 \end{pmatrix}. \tag{2.4}$$

To obtain the L^2 estimate, we multiply the equation with $\mathbf{B}$ and then we integrate over $\mathbb{R}^3$ resulting in

$$\begin{aligned}\int_{\mathbb{R}^3} \frac{1}{2}\frac{\partial \mathbf{B}^2}{\partial t} + \left(\frac{\delta_e}{L_0}\right)^2 \frac{1}{\rho}\mathbf{B}\nabla \times (\nabla \times \frac{\partial \mathbf{B}}{\partial t})dx &= \int_{\mathbb{R}^3} [\mathbf{B}^\top C\mathbf{B} - (\nabla \cdot \mathbf{u})\mathbf{B} - \frac{1}{2}(\mathbf{u} \cdot \nabla)\mathbf{B}^2 - \eta \mathbf{B}\nabla \times (\nabla \times \mathbf{B}) \\ &- \left(\frac{\delta_e}{L_0}\right)^2 \frac{1}{\rho}\mathbf{B}\nabla \times ((\mathbf{u} \cdot \nabla)(\nabla \times \mathbf{B})) - \frac{\delta_i}{L_0}\frac{1}{\rho}\mathbf{B}\nabla \times ((\nabla \times \mathbf{B}) \times \mathbf{B})]dx.\end{aligned}$$

Partial integration yields

$$\begin{aligned}&\frac{1}{2}\frac{d}{dt}\left(\|\mathbf{B}\|^2_{L^2(\mathbb{R}^3)} + \left(\frac{\delta_e}{L_0}\right)^2 \frac{1}{\rho}\|\nabla \times \mathbf{B}\|^2_{L^2(\mathbb{R}^3)}\right) = \\ &\int_{\mathbb{R}^3} [\mathbf{B}^\top C\mathbf{B} - \frac{1}{2}(\nabla \cdot \mathbf{u})\mathbf{B}^2 - \eta(\nabla \times \mathbf{B})^2 + \frac{1}{2}\left(\frac{\delta_e}{L_0}\right)^2 \frac{1}{\rho}(\nabla \cdot \mathbf{u})(\nabla \times \mathbf{B})^2 - \frac{\delta_i}{L_0}\frac{1}{\rho}\underbrace{(\nabla \times \mathbf{B})((\nabla \times \mathbf{B}) \times \mathbf{B})}_{=0}]dx\end{aligned}$$

$$= \int_{\mathbb{R}^3} [\mathbf{B}^\top C\mathbf{B} - \frac{1}{2}(\nabla\cdot\mathbf{u})\mathbf{B}^2 - \eta(\nabla\times\mathbf{B})^2 + \frac{1}{2}\left(\frac{\delta_e}{L_0}\right)^2 \frac{1}{\rho}(\nabla\cdot\mathbf{u})(\nabla\times\mathbf{B})^2]dx.$$

We did not consider the boundary terms because they vanish since the solution B is decaying to zero at infinity. Using Cauchy-Schwartz we obtain

$$\frac{1}{2}\frac{d}{dt}\left(\|\mathbf{B}\|^2_{L^2(\mathbb{R}^3)} + \left(\frac{\delta_e}{L_0}\right)^2 \|\nabla\times\mathbf{B}\|^2_{L^2(\mathbb{R}^3)}\right) \leq \frac{1}{2}\left(C_A\|\mathbf{B}\|^2_{L^2\mathbb{R}^3} + C_B\left(\frac{\delta_e}{L_0}\right)^2 \frac{1}{\rho}\|\nabla\times\mathbf{B}\|^2_{L^2\mathbb{R}^3}\right)$$

where $C_A \max_{k,i}\left(\left\|\frac{\partial u_i}{\partial x_k}\right\|_{L^\infty(\mathbb{R}^3)}\right)$ and $C_B = \|\nabla\cdot\mathbf{u}\|_{L^\infty(\mathbb{R}^3)}$. □

We have shown that the induction equation in symmetric form possesses an energy estimate. However, the divergence of the solution of (1.11) is not preserved exactly. Nevertheless, we have the following estimate:

Theorem 2.2. *Let $\mathbf{u} \in C^2(\mathbb{R}^3)$ Furthermore, assume that the divergence of the solution of (2.2), $\nabla\cdot\mathbf{B}$, decays to zero at infinity, then the following apriori estimate holds:*

$$\frac{d}{dt}\|\nabla\cdot\mathbf{B}\|_{L^2(\mathbb{R}^3)} \leq C\|\nabla\cdot\mathbf{B}\|_{L^2(\mathbb{R}^3)} \tag{2.5}$$

with C being a constant that depend on $\mathbf{u}$ and its derivatives only.

Proof. Applying the divergence operator on (2.2) we obtain

$$\frac{\partial\,\nabla\cdot\mathbf{B}}{\partial t} = -\nabla\cdot(\mathbf{u}(\nabla\cdot\mathbf{B})) \tag{2.6}$$

using vector identity we can rewrite the right hand side of the equation

$$\frac{\partial\,\nabla\cdot\mathbf{B}}{\partial t} = -\mathbf{u}\cdot\nabla(\nabla\cdot\mathbf{B}) - (\nabla\cdot\mathbf{B})(\nabla\cdot\mathbf{u}).$$

Multiplying this equation by $\nabla\cdot\mathbf{B}$ and integrating it over $\mathbb{R}^3$ we obtain

$$\frac{1}{2}\frac{d}{dt}\|\nabla\cdot\mathbf{B}\|_{L^2(\mathbb{R}^3)} = -\frac{1}{2}\int_{\mathbb{R}^3}\mathbf{u}\cdot(\nabla(\nabla\cdot\mathbf{B})^2)dx - \int_{\mathbb{R}^3}(\nabla\cdot\mathbf{u})(\nabla\cdot\mathbf{B})^2dx,$$

with partial integration we obtain

$$\begin{aligned}\frac{1}{2}\frac{d}{dt}\|\nabla\cdot\mathbf{B}\|_{L^2(\mathbb{R}^3)} &= \frac{1}{2}\int_{\mathbb{R}^3}(\nabla\cdot\mathbf{u})(\nabla\cdot\mathbf{B})^2dx - \frac{1}{2}\int_{\mathbb{R}^3}(\mathbf{u}\cdot\mathbf{n})(\nabla\cdot\mathbf{B})^2ds \\ &\leq \frac{1}{2}\|\nabla\cdot\mathbf{u}\|_{L^\infty(\mathbb{R}^3)}\|\nabla\cdot\mathbf{B})\|^2_{L^2(\mathbb{R}^3)}.\end{aligned}$$

□

Corollary 2.1. *If the conditions for theorems theorem. 2.1 and theorem. 2.2 hold and the initial data $\mathbf{B} \in H^1(\mathbb{R}^3)$, then the estimates imply that $\mathbf{B} \in L^\infty((0,T), H^1(\mathbb{R}^3))$.*

Remark 2.1. *The divergence transport equation* (2.6) *implies that the divergence remains zero if the initial data has zero divergence. In this case, the solutions of the symmetric form* (2.2) *are also weak solutions of the non-symmetric form* (1.11) *of the Hall induction equations.*

3. Numerical Scheme

In this section, we design numerical schemes that satisfy a discrete version of the energy estimates of the last section. The computational domain is $\Omega = [0, L_x] \times [0, L_y] \times [0, L_z]$ and we define a uniform mesh of N_x times N_y times N_z points with coordinates $x_i = i\Delta x$, $y_j = j\Delta y$ and $z_k = k\Delta z$. In this case $\Delta x = L_x/(N_x - 1)$, $\Delta y = L_y/(N_y - 1)$ and $\Delta z = L_z/(N_z - 1)$ are mesh widths.

The point values of the magnetic and velocity fields are

$$\tilde{\mathbf{B}}_{i,j,k} \sim \mathbf{B}(x_i, y_j, z_k) \quad \tilde{\mathbf{u}}_{i,j,k} \sim \mathbf{u}(x_i, y_j, z_k).$$

We will provide a very general discrete formulation and specify the necessary requirement that the discrete derivative should posses. As in [6, 5, 8], the key requirement for the discrete derivative is to satisfy a summation by parts (SBP) condition. The exact form of operators satisfying the requirements are presented in appendix A.

We start with one dimensional discrete derivatives using grid functions in vector form, i.e., $w = (w_0, \cdots w_{N_x-1})^\top$. An approximation of the x spatial derivative, D_x possesses the summation by parts property (see [11]) if it can be written as $D_x = P_x^{-1}Q_x$, where P_x is a diagonal $N_x \times N_x$ positive definite matrix and Q_x an $N_x \times N_x$ matrix satisfying:

$$Q_x + Q_x^\top = R_{N_x} - L_{N_x} \tag{3.1}$$

where R_{N_x} and L_{N_x} are $N_x \times N_x$ matrices: diag(0,$\cdots$,0,1) and diag(1,0,$\cdots$,0).
The operator P defines an inner product

$$(v, w)_{P_x} = v^\top P_x w \tag{3.2}$$

with the associated norm $\|w\|_P = (w, w)_{P_x}^{1/2}$ that is equivalent to the norm $\|w\| = (\Delta x \sum_k w_k^2)^{1/2}$.
Next, we define averaging operators such that we can obtain an approximate form of the chain rule.

We define symmetric averaging operators as

$$(A_x w)_i = \sum_{k=-r}^{q} \alpha_k w_{i+k} \tag{3.3}$$

with $\sum_{k=-r}^{q} \alpha_k = 1$ and $\alpha_{-i} = \alpha_i$.
In [8], the following discrete chain rule was shown,

Lemma 3.1. *Given any smooth function $u(x)$, we denote his restriction on the grid as $\bar{u}$ and let be w a grid function. Then we can define an average operator $\bar{A}_x$ coupled to D_x such that*

$$D_x(\bar{u} \circ w) = \bar{u} \circ D_x(w) + D_x(\bar{u}) \circ \bar{A}_x(w) + \tilde{w}, \tag{3.4}$$

where $(u \circ w)_{i,j,k} = u_{i,j,k} w_{i,j,k}$ and with $\bar{A}_x(w) = \sum_{k=-r}^{q} k\beta_k w_{i+k}$ and $\|\tilde{w}\|_P \leq C\Delta x \|w\|_P$.

Proof. The discrete differential operator acting on a grid function w_i can also be written through sums:

$$(D_x w)_i = \frac{1}{\Delta x} \sum_{k=-r}^{q'} \beta_{k'} w_{i+k}.$$

with $\sum_{k=-r}^{q} \beta_k = 0$ and $\sum_{k=-r}^{q} k\beta_k = 1$. Then the residual $\tilde{w}$ is given by

$$\begin{aligned}
\tilde{w}_i &= D_x(\bar{u} \circ w)_i - (\bar{u} \circ D_x w)_i - (D_x(\bar{u}) \circ \bar{A}_x(w))_i \\
&= \frac{1}{\Delta x} \sum_{k=-r}^{q} \beta_k \bar{u}_{i+k} w_{i+k} - \frac{\bar{u}_i}{\Delta x} \sum_{k=-r}^{q} \beta_k w_{i+k} - \frac{1}{\Delta x} \left(\sum_{l=-r}^{q} \beta_l \bar{u}_{i+l} \right) \sum_{k=-r}^{q} k\beta_k w_{i+k}.
\end{aligned}$$

We expand $\bar{u}$ with Taylor-expansion

$$\bar{u}_{i+k} = \bar{u}_i + \Delta x k \bar{u}_i' + \frac{1}{2} \Delta x^2 k^2 \mathfrak{c}_k^i$$

where $\mathfrak{c}_k^i = \bar{u}_i''(\xi_k)$ obtaining

$$\begin{aligned}
\tilde{w}_i = &\frac{\bar{u}_i}{\Delta x} \bar{u}_i \sum_{k=-r}^{q} \beta_k w_{i+k} + \bar{u}_i' \sum_{k=-r}^{q} k\beta_k w_{i+k} + \Delta x \sum_{k=-r}^{q} k^2 \beta_k c_k^i w_{i+k} - \frac{\bar{u}_i}{\Delta x} \bar{u}_i \sum_{k=-r}^{q} \beta_k w_{i+k} \\
&- \left(\bar{u}_i' + \Delta x \sum_{l=-r}^{q} l^2 \beta_l c_l^i \right) \sum_{k=-r}^{q} k\beta_k w_{i+k} = \Delta x \sum_{k=-r}^{q} \gamma_k^i w_{i+k}.
\end{aligned}$$

Here $\gamma_k^i = k\beta_k \frac{k\mathfrak{c}_k - \sum_{l=-r}^{q} l^2 \beta_l c_l^i}{2}$. Since the γ_k^i are bounded, we have that

$$\|\tilde{w}\|_{P_x} \leq \Delta x C \|w\|_{P_x}$$

where C depends only on the maximum of γ_k^i and on the norm P_x. □

We show the following lemma claiming that differential operators commute with average operators,

Lemma 3.2. *The discrete differential operator D_x and the average operator A_x commute.*

Proof. We write the discrete differential operator acting on a grid function w_i through sums:

$$(D_x w)_i = \frac{1}{\Delta x} \sum_{k'=-r'}^{q'} \beta_{k'}.w_{i+k'}.$$

Then applying the two operators consecutively we obtain

$$\begin{aligned}(D_x(A_x w))_i &= \frac{1}{\Delta x} \sum_{k'=-r'}^{q'} \beta_{k'} (A_x w)_{i+k'} = \frac{1}{\Delta x} \sum_{k'=-r'}^{q'} \beta_{k'} \sum_{k=-r}^{q} \alpha_k w_{i+k'+k} \\ &= \frac{1}{\Delta x} \sum_{k'=-r'}^{q'} \sum_{k=-r}^{q} \beta_{k'} \alpha_k w_{i+k'+k} = \frac{1}{\Delta x} \sum_{k=-r}^{q} \sum_{k'=-r'}^{q'} \beta_{k'} \alpha_k w_{i+k'+k} \\ &= \frac{1}{\Delta x} \sum_{k=-r}^{q} \alpha_k \sum_{k'=-r'}^{q'} \beta_{k'} w_{i+k'+k} = \sum_{k=-r}^{q} \alpha_k (D_x w)_{i+k} = (A_x(D_x w))_i\end{aligned}$$

□

We use the above one dimensional operators to build the multidimensional operators i.e, mappings of three dimensional grid functions $w(x_i, y_j, z_k) = w_{i,j.k}$ to a column vector

$$w = (w_{0,0,0}, w_{0,0,1}, \cdots, w_{0,0,N_z}, w_{0,1,0}, \cdots, w_{N_x,N_y,N_z})^\top. \tag{3.5}$$

We define the discrete differential operators and averages

$$\begin{aligned}\mathfrak{d}_x &= D_x \otimes A_y \otimes A_z, \\ \mathfrak{d}_y &= A_x \otimes D_y \otimes A_z, \\ \mathfrak{d}_z &= A_x \otimes A_y \otimes D_z, \\ \mathcal{A}_x &= \bar{A}_x \otimes A_y \otimes A_z, \\ \mathcal{A}_y &= A_x \otimes \bar{A}_y \otimes A_z, \\ \mathcal{A}_z &= A_x \otimes A_y \otimes \bar{A}_z.\end{aligned}$$

Here $\otimes$ is the Kronecker product. We also extend the inner product by $\mathbf{P} = \mathbf{P_x} \otimes \mathbf{P_y} \otimes \mathbf{P_z}$ with the corresponding norm $\|w\|_{\mathbf{P}} = (w, w)_{\mathbf{P}}^{1/2}$.

We generalize the one dimensional operators to three dimensions using the average operators A_x, A_y and A_z. Setting the averaging operators to the identity mapping allows us to recover the *standard* version of one dimensional discrete operators. However, we will use a more general form of the averaging operator that will allow us to include a larger group of difference operators including the divergence preserving operators of [12] and some of the divergence preserving operators proposed in [9].

We can expand lemma 3.1 in three dimensions:

Corollary 3.1. *Given any smooth function $\bar{u}(x)$ as above, then*

$$\|\mathfrak{d}_x(u \circ w) - u \circ \mathfrak{d}_x w\|_{\mathbf{P}} \leq C \|w\|_{\mathbf{P}} \tag{3.6}$$

where C a constant which depends on the first order derivative of u.

Proof. The proof of this corollary is similar to the one done before only using a substitution with a Taylor expansion of degree one. □

The summation by parts property of the differential operators, coupled with the inner product $\mathbf{P}$ will result in a discrete version on integration by parts:

Lemma 3.3. *For any gird function v and w, we have*

$$\begin{aligned}(v,\mathfrak{d}_x w)_{\mathbf{P}}+(\mathfrak{d}_x v,w)_{\mathbf{P}}&=v^\top(\mathcal{R}-\mathcal{L})w,\\(v,\mathfrak{d}_y w)_{\mathbf{P}}+(\mathfrak{d}_y v,w)_{\mathbf{P}}&=v^\top(\mathcal{U}-\mathcal{D})w,\\(v,\mathfrak{d}_z w)_{\mathbf{P}}+(\mathfrak{d}_z v,w)_{\mathbf{P}}&=v^\top(\mathcal{T}-\mathcal{B})w\end{aligned}\tag{3.7}$$

where $\mathcal{R}=R_{N_x}\otimes P_yA_y\otimes P_zA_z$, $\mathcal{L}=L_{N_x}\otimes P_yA_y\otimes P_zA_z$, $\mathcal{U}=P_xA_x\otimes R_{N_y}\otimes P_zA_z$, $\mathcal{D}=P_xA_y\otimes L_{R_y}\otimes P_zA_z$, $\mathcal{T}=P_xA_y\otimes P_yA_y\otimes R_{N_z}$ *and* $\mathcal{B}=P_xA_y\otimes P_yA_y\otimes L_{N_z}$.

Proof. Since A_k's are symmetric and P_k's diagonal, we can calculate

$$\begin{aligned}(v,\mathfrak{d}_x w)_{\mathbf{P}}+(\mathfrak{d}_x v,w)_{\mathbf{P}}=&\\&v^\top(P_x\otimes P_y\otimes P_z)(P_x^{-1}Q_x\otimes A_y\otimes A_z)w+((P_x^{-1}Q_x\otimes A_y\otimes A_z)v)^\top(P_x\otimes P_y\otimes P_z)w=\\&v^\top(Q_x\otimes A_y^\top P_y\otimes A_z^\top P_z)w+v^\top(Q_x^\top\otimes P_yA_y\otimes P_zA_z)w=\\&v^\top((Q_x^\top+Q_x)\otimes P_yA_y\otimes P_zA_z)w=\\&v^\top(R_{N_x}\otimes P_yA_y\otimes P_zA_z)w-v^\top(L_{N_x}\otimes P_yA_y\otimes P_zA_z)w.\end{aligned}$$

The proof for the other space directions follow analogously. □

The right hand side of the above equation represents the evaluation of the grid function on the boundary of Ω.

Until now all our analysis was for scalar operators, we extend it to vector-valued discrete differential operators below.

Corollary 3.2. *We derive from the scalar summation by parts rules for scalar fields*

$$\begin{aligned}(\tilde{\mathbf{v}},\mathbf{D}\cdot\tilde{\mathbf{w}})_{\mathbf{P}}&=-(\mathbf{D}\tilde{\mathbf{v}},\tilde{\mathbf{w}})_{\mathbf{P}}+\sum_i\hat{v}_i\mathcal{S}_i\hat{w}_i,\\(\tilde{\mathbf{v}},\mathbf{D}\times\tilde{\mathbf{w}})_{\mathbf{P}}&=(\mathbf{D}\times\tilde{\mathbf{v}},\tilde{\mathbf{w}})_{\mathbf{P}}+\sum_{i,j,k}\epsilon_{i,j,k}\hat{v}_i\mathcal{S}_j\hat{w}_k\end{aligned}\tag{3.8}$$

where $\mathbf{D}=(\mathfrak{d}_x,\mathfrak{d}_y,\mathfrak{d}_z)^\top$, $\mathcal{S}_1=\mathcal{L}-\mathcal{R}$, $\mathcal{S}_2=\mathcal{U}-\mathcal{D}$, $\mathcal{S}_3=\mathcal{T}-\mathcal{B}$ *and* $\epsilon_{i,j,k}$ *is the Levi-Civita symbol.*

Proof. The proof of this corollary is given by the direct application of the previous theorem on discrete vector fields. □

In the continuous case, the key property for the preservation of divergence is the identity:

$$\nabla\cdot(\nabla\times\mathbf{w})=0$$

for all $\mathbf{w}\in(C^2(\mathbb{R}^3))^3$. From Lemma (3.2) and the definition of Kronecker product, one observes that the difference operators $\mathfrak{d}_x,\mathfrak{d}_y$ and $\mathfrak{d}_z$ commute, we can show that is also the case for the discrete differential operator:

Corollary 3.3. *Every grid function* $\hat{\mathbf{w}}_{i,j,k}$ *coupled with* $\mathbf{D}=(\mathfrak{d}_x,\mathfrak{d}_y,\mathfrak{d}_z)^\top$ *satisfies*

$$\mathbf{D}\cdot(\mathbf{D}\times\hat{\mathbf{w}})=0.\tag{3.9}$$

The proof of this corollary is straightforward.
Generalizing lemma 3.3 presented in [6] for the vector operator $\mathbf{D}$:

Lemma 3.4. *If* $\tilde{\mathbf{u}}$ *is a vector grid function*

$$(\mathbf{v},(\tilde{\mathbf{u}}\cdot\mathbf{D})\circ\tilde{\mathbf{v}})_{\mathbf{P}}=\frac{1}{2}\left(\tilde{\mathbf{v}},(\tilde{\mathbf{u}}\mathbf{D})\circ\tilde{\mathbf{v}}-\sum_i\mathbf{D}((\tilde{\mathbf{u}}^i)\circ\tilde{\mathbf{v}})\right)_{\mathbf{P}}+\frac{1}{2}\sum_i\tilde{\mathbf{v}}^\top\mathcal{S}_i((\tilde{\mathbf{u}}^i)\circ\tilde{\mathbf{v}})\tag{3.10}$$

Proof. See the proof in [5] and apply it on each component of $\tilde{\mathbf{u}}\cdot\tilde{\mathbf{D}}$. □

Now we have all the ingredients to present two different classes of numerical schemes. The first set of schemes termed as *symmetric schemes* will discretize the symmetric version of the Hall magnetic induction equation (2.2). The second set of schemes will discrete the non-symmetric version (1.11) of the Hall induction equations and will preserve a discrete version of divergence. Hence, we term it *divergence preserving scheme*.

3.1. **Symmetric Scheme.** We discretize the symmetric form (2.2) of the Hall induction equations and definie a semi-discrete numerical scheme as

$$\frac{d}{dt}\left(\tilde{\mathbf{B}}_{i,j,k}+\left(\frac{\delta_e}{L_0}\right)^2\frac{1}{\rho}(\mathbf{D}\times\mathbf{D}\times\tilde{\mathbf{B}})_{i,j,k}\right)=\mathcal{AV}(\tilde{\mathbf{B}},\tilde{\mathbf{u}})-(\tilde{\mathbf{u}}_{i,j,k}\cdot\mathbf{D})\tilde{\mathbf{B}}_{i,j,k}-\eta(\mathbf{D}\times(\mathbf{D}\times\tilde{\mathbf{B}}_{i,j,k}))$$
$$-\left(\frac{\delta_e}{L_0}\right)^2\frac{1}{\rho}\mathbf{D}\times((\tilde{\mathbf{u}}_{i,j,k}\cdot\mathbf{D})(\mathbf{D}\times\tilde{\mathbf{B}}_{i,j,k}))-\frac{\delta_i}{L_0}\frac{1}{\rho}\mathbf{D}\times((\mathbf{D}\times\tilde{\mathbf{B}}_{i,j,k})\times\tilde{\mathbf{B}}_{i,j,k}) \tag{3.11}$$

where

$$\mathcal{AV}(\tilde{\mathbf{B}},\tilde{\mathbf{u}})=(\bar{\mathcal{A}}(\tilde{\mathbf{B}}_{i,j,k})\cdot\mathbf{D})\tilde{\mathbf{u}}_{i,j,k}-\bar{\mathcal{A}}_x(\tilde{\mathbf{B}}_{i,j,k})\mathfrak{d}_x(\tilde{\mathbf{u}}^1_{i,j,k})-\bar{\mathcal{A}}_y(\tilde{\mathbf{B}}_{i,j,k})\mathfrak{d}_y(\tilde{\mathbf{u}}^2_{i,j,k})-\bar{\mathcal{A}}_z(\tilde{\mathbf{B}}_{i,j,k})\mathfrak{d}_z(\tilde{\mathbf{u}}^3_{i,j,k}), \tag{3.12}$$

$$\bar{\mathcal{A}}(\tilde{\mathbf{B}}_{i,j,k})=(\bar{\mathcal{A}}_x(\tilde{\mathbf{B}}^1_{i,j,k}),\bar{\mathcal{A}}_y(\tilde{\mathbf{B}}^2_{i,j,k}),\bar{\mathcal{A}}_z(\tilde{\mathbf{B}}^3_{i,j,k}))^\top. \tag{3.13}$$

The term $\mathcal{AV}$ represent the discretisation of $(\mathbf{B}\cdot\nabla)\mathbf{u}-\mathbf{B}(\nabla\cdot\mathbf{u})$. We estimate it below,

Lemma 3.5. *For $\tilde{\mathbf{B}}_{i,j,k}$ gird function and $\tilde{\mathbf{u}}_{i,j,k}$ a bounded grid function, we have*

$$(\tilde{\mathbf{B}},\mathcal{AV}(\tilde{\mathbf{B}},\tilde{\mathbf{u}}))_{\mathbf{P}}\leq C\|\tilde{\mathbf{B}}\|^2_{\mathbf{P}} \tag{3.14}$$

where C depends on $\tilde{\mathbf{u}}$ and its discrete derivative only.

Proof. We write (3.14) component-wise and using the triangle inequality, we obtain

$$\begin{aligned}(\tilde{\mathbf{B}},\mathcal{AV}(\tilde{\mathbf{B}},\tilde{\mathbf{u}}))_{\mathbf{P}}\leq&\sum_{i=1}^3|(\tilde{\mathbf{B}^i},\bar{\mathcal{A}}_x(\tilde{\mathbf{B}}^1)\mathfrak{d}_x\tilde{\mathbf{u}}^i)_{\mathbf{P}}|+|(\tilde{\mathbf{B}^i},\bar{\mathcal{A}}_y(\tilde{\mathbf{B}}^2)\mathfrak{d}_y\tilde{\mathbf{u}}^i)_{\mathbf{P}}|+|(\tilde{\mathbf{B}^i},\bar{\mathcal{A}}_z(\tilde{\mathbf{B}}^3)\mathfrak{d}_z\tilde{\mathbf{u}}^i)_{\mathbf{P}}|\\&+|(\tilde{\mathbf{B}^i},\bar{\mathcal{A}}_x(\tilde{\mathbf{B}}^i)\mathfrak{d}_x\tilde{\mathbf{u}}^1)_{\mathbf{P}}|+|(\tilde{\mathbf{B}^i},\bar{\mathcal{A}}_y(\tilde{\mathbf{B}}^i)\mathfrak{d}_y\tilde{\mathbf{u}}^2)_{\mathbf{P}}|+|(\tilde{\mathbf{B}^i},\bar{\mathcal{A}}_z(\tilde{\mathbf{B}}^i)\mathfrak{d}_z\tilde{\mathbf{u}}^3)_{\mathbf{P}}|.\end{aligned}$$

Since the discrete derivative of $\tilde{\mathbf{u}}$ are bounded, we can extract its maximum from the $\mathbf{P}$ norms and obtain

$$\begin{aligned}(\tilde{\mathbf{B}},\mathcal{AV}(\tilde{\mathbf{B}},\tilde{\mathbf{u}}))_{\mathbf{P}}\leq&C\sum_{i=1}^3|(\tilde{\mathbf{B}^i},\bar{\mathcal{A}}_x(\tilde{\mathbf{B}}^1))_{\mathbf{P}}|+|(\tilde{\mathbf{B}^i},\bar{\mathcal{A}}_y(\tilde{\mathbf{B}}^2))_{\mathbf{P}}|+|(\tilde{\mathbf{B}^i},\bar{\mathcal{A}}_z(\tilde{\mathbf{B}}^3))_{\mathbf{P}}|+|(\tilde{\mathbf{B}^i},\bar{\mathcal{A}}_x(\tilde{\mathbf{B}}^i))_{\mathbf{P}}|\\&+|(\tilde{\mathbf{B}^i},\bar{\mathcal{A}}_y(\tilde{\mathbf{B}}^i))_{\mathbf{P}}|+|(\tilde{\mathbf{B}^i},\bar{\mathcal{A}}_z(\tilde{\mathbf{B}}^i))_{\mathbf{P}}|\\\leq&C\Big(2\Big(|(\tilde{\mathbf{B}^1},\bar{\mathcal{A}}_x(\tilde{\mathbf{B}}^1))_{\mathbf{P}}|+|(\tilde{\mathbf{B}^2},\bar{\mathcal{A}}_y(\tilde{\mathbf{B}}^2))_{\mathbf{P}}|+|(\tilde{\mathbf{B}^3},\bar{\mathcal{A}}_z(\tilde{\mathbf{B}}^3))_{\mathbf{P}}|\Big)+|(\tilde{\mathbf{B}^2},\bar{\mathcal{A}}_x(\tilde{\mathbf{B}}^1))_{\mathbf{P}}|\\&+|(\tilde{\mathbf{B}^3},\bar{\mathcal{A}}_x(\tilde{\mathbf{B}}^1))_{\mathbf{P}}|+|(\tilde{\mathbf{B}^1},\bar{\mathcal{A}}_y(\tilde{\mathbf{B}}^2))_{\mathbf{P}}|+|(\tilde{\mathbf{B}^3},\bar{\mathcal{A}}_y(\tilde{\mathbf{B}}^2))_{\mathbf{P}}|+|(\tilde{\mathbf{B}^1},\bar{\mathcal{A}}_z(\tilde{\mathbf{B}}^3))_{\mathbf{P}}|\\&+|(\tilde{\mathbf{B}^2},\bar{\mathcal{A}}_z(\tilde{\mathbf{B}}^3))_{\mathbf{P}}|\Big)\end{aligned}$$

Take the first term and first use the equivalence of inner product, then write the average operator through summation, and finally using the Cauchy inequality yields

$$\begin{aligned}|(\tilde{\mathbf{B}^1},\bar{\mathcal{A}}_x(\tilde{\mathbf{B}}^1))_{\mathbf{P}}|\leq C|(\tilde{\mathbf{B}^1},\bar{\mathcal{A}}_x(\tilde{\mathbf{B}}^1))|&=C|\sum_{i,j,k,l}\tilde{\mathbf{B}^1}_{i,j,k}\alpha_l\tilde{\mathbf{B}^1}_{i,j+l,k}|\\&\leq C\frac{\max_l(\alpha_l)}{2}\sum_{i,j,k,l}[(\tilde{\mathbf{B}^1}_{i,j,k})^2+(\tilde{\mathbf{B}^1}_{i,j+l,k})^2]\leq C\|\tilde{\mathbf{B}}\|^2.\end{aligned}$$

Repeating this procedure for all the term of the sum, yields to

$$(\tilde{\mathbf{B}},\mathcal{AV}(\tilde{\mathbf{B}},\tilde{\mathbf{u}}))_{\mathbf{P}}\leq C\|\tilde{\mathbf{B}}\|^2.$$

The use of the equivalence between Euclidean and $\mathbf{P}$ norms conclude the proof of lemma. □

This lemma will allow us to is now prove the energy stability of the scheme. The main theorem is:

Theorem 3.1. *Let $\tilde{\mathbf{u}}_{i,j,k} = \mathbf{u}(x_i, y_j, z_k)$ be the point evaluation of a function $u \in C^2$ and let the approximate solutions $\tilde{\mathbf{B}}$ of (3.11) go to zero at infinity, then the following estimates hold*

$$\frac{d}{dt}\left(\|\tilde{\mathbf{B}}\|^2_{\mathbf{P}} + \left(\frac{\delta_e}{L_0}\right)^2 \frac{1}{\rho}\|\mathbf{D}\times\tilde{\mathbf{B}}\|^2_{\mathbf{P}}\right) \leq C\left(\|\tilde{\mathbf{B}}\|^2_{\mathbf{P}} + \left(\frac{\delta_e}{L_0}\right)^2 \frac{1}{\rho}\|\mathbf{D}\times\tilde{\mathbf{B}}\|^2_{\mathbf{P}}\right) \tag{3.15}$$

with C a constant that depend on $\mathbf{u}$ and its derivative only.

Proof. Multiplying both sides of the scheme (3.11) by $\tilde{\mathbf{B}}$ yields

$$\begin{aligned}\frac{1}{2}\frac{d}{dt}\|\tilde{\mathbf{B}}\|^2_{\mathbf{P}} + \left(\frac{\delta_e}{L_0}\right)^2 \frac{1}{\rho}(\tilde{\mathbf{B}}, (\mathbf{D}\times\mathbf{D}\times\frac{d}{dt}\tilde{\mathbf{B}}))_{\mathbf{P}} &= (\tilde{\mathbf{B}}, \mathcal{AV}(\tilde{\mathbf{B}}, \tilde{\mathbf{u}}))_{\mathbf{P}} - (\tilde{\mathbf{B}}, (\tilde{\mathbf{u}}\cdot\mathbf{D})\circ\tilde{\mathbf{B}})_{\mathbf{P}} - \eta(\tilde{\mathbf{B}}, \mathbf{D}\times(\mathbf{D}\times\tilde{\mathbf{B}}))_{\mathbf{P}} \\ &- \left(\frac{\delta_e}{L_0}\right)^2 \frac{1}{\rho}(\tilde{\mathbf{B}}, \mathbf{D}\times((\tilde{\mathbf{u}}\cdot\mathbf{D})\circ(\mathbf{D}\times\tilde{\mathbf{B}}))_{\mathbf{P}} - \frac{\delta_i}{L_0}\frac{1}{\delta}(\tilde{\mathbf{B}}, \mathbf{D}\times((\mathbf{D}\times\tilde{\mathbf{B}})\times\tilde{\mathbf{B}}))_{\mathbf{P}}.\end{aligned}$$

Using summation by parts of corollary 3.2 and lemma 3.4

$$\begin{aligned}\frac{d}{dt}\frac{1}{2}\left(\|\tilde{\mathbf{B}}\|^2_{\mathbf{P}} + \left(\frac{\delta_e}{L_0}\right)^2 \frac{1}{\rho}\|\mathbf{D}\times\tilde{\mathbf{B}}\|^2_{\mathbf{P}}\right) &= (\tilde{\mathbf{B}}, \mathcal{AV}(\tilde{\mathbf{B}}, \tilde{\mathbf{u}}))_{\mathbf{P}} - \frac{1}{2}(\tilde{\mathbf{B}}, (\tilde{\mathbf{u}}\cdot\mathbf{D})\circ\tilde{\mathbf{B}} - \sum_i \mathbf{D}(\tilde{\mathbf{u}}^i\circ\tilde{\mathbf{B}}))_{\mathbf{P}} \\ &- \eta\|\mathbf{D}\times\tilde{\mathbf{B}}\|^2_{\mathbf{P}} - \left(\frac{\delta_e}{L_0}\right)^2 \frac{1}{\rho}(\mathbf{D}\times\tilde{\mathbf{B}}, (\tilde{\mathbf{u}}\cdot\mathbf{D})\circ(\mathbf{D}\times\tilde{\mathbf{B}}))_{\mathbf{P}} - \frac{\delta_i}{L_0}\frac{1}{\delta}\underbrace{(\mathbf{D}\times\tilde{\mathbf{B}}, (\mathbf{D}\times\tilde{\mathbf{B}})\times\tilde{\mathbf{B}})_{\mathbf{P}}}_{=0} = \\ &(\tilde{\mathbf{B}}, \mathcal{AV}(\tilde{\mathbf{B}}, \tilde{\mathbf{u}}))_{\mathbf{P}} - \frac{1}{2}(\tilde{\mathbf{B}}, (\tilde{\mathbf{u}}\cdot\mathbf{D})\circ\tilde{\mathbf{B}} - \sum_i \mathbf{D}(\tilde{\mathbf{u}}^i\circ\tilde{\mathbf{B}}))_{\mathbf{P}} - \eta\|\mathbf{D}\times\tilde{\mathbf{B}}\|^2_{\mathbf{P}} \\ &- \left(\frac{\delta_e}{L_0}\right)^2 \frac{1}{\rho}(\mathbf{D}\times\tilde{\mathbf{B}}, (\tilde{\mathbf{u}}\cdot\mathbf{D})\circ(\mathbf{D}\times\tilde{\mathbf{B}}) - \sum_i \mathbf{D}(\tilde{\mathbf{u}}^i\circ(\mathbf{D}\times\tilde{\mathbf{B}})))_{\mathbf{P}}.\end{aligned}$$

All the boundary terms have been neglected since the data decay to 0 at infinity.
Using lemma 3.4 and lemma 3.5 we obtain

$$\frac{d}{dt}\frac{1}{2}\left(\|\tilde{\mathbf{B}}\|^2_{\mathbf{P}} + \left(\frac{\delta_e}{L_0}\right)^2 \frac{1}{\rho}\|\mathbf{D}\times\tilde{\mathbf{B}}\|^2_{\mathbf{P}}\right) \leq C_1\left(\|\tilde{\mathbf{B}}\|^2_{\mathbf{P}} + \left(\frac{\delta_e}{L_0}\right)^2 \frac{1}{\rho}\|\mathbf{D}\times\tilde{\mathbf{B}}\|^2_{\mathbf{P}}\right).$$

□

Since the divergence is not preserved by the symmetric scheme, we show that the divergence generated by the symmetric scheme is bounded (a similar result for the ideal magnetic induction equations was shown in [8]).

Theorem 3.2. *Let $\tilde{\mathbf{u}}_{i,j,k} = \mathbf{u}(x_i, y_j, z_k)$ be the point evaluation of a function $u \in C^2$ and let the solutions of (3.11) go to zero at infinity, then the following estimates hold*

$$\frac{d}{dt}\|\mathbf{D}\cdot\tilde{\mathbf{B}}\|^2_{\mathbf{P}} \leq C(\|\mathbf{D}\cdot\tilde{\mathbf{B}}\|^2_{\mathbf{P}} + \|\tilde{\mathbf{B}}\|^2) \tag{3.16}$$

with C a constant that depend on $\mathbf{u}$ and and its derivative and on the regularity of the grid.

Proof. We define the discrete divergence $\hat{\omega} = \mathbf{D}\cdot\tilde{\mathbf{B}}$ and using the numerical scheme (3.11) with corollary 3.3, we obtain an equation for its evolution

$$\frac{d}{dt}\hat{\omega} = \mathbf{D}\cdot(\mathcal{AV}(\tilde{\mathbf{B}}, \tilde{\mathbf{u}}) - (\tilde{\mathbf{u}}\circ\mathbf{D})\tilde{\mathbf{B}}).$$

Now expanding each component of $\mathcal{AV}$ and using lemma 3.1, we obtain, for example for the first component:

$$\begin{aligned}(\mathcal{AV}(\tilde{\mathbf{B}}, \tilde{\mathbf{u}}))^1 &= \bar{\mathcal{A}}_y(\tilde{\mathbf{B}}^2)\circ\mathfrak{d}_y\tilde{\mathbf{u}}^1 + \bar{\mathcal{A}}_z(\tilde{\mathbf{B}}^3)\circ\mathfrak{d}_z\tilde{\mathbf{u}}^1 - \bar{\mathcal{A}}_y(\tilde{\mathbf{B}}^1)\circ\mathfrak{d}_y\tilde{\mathbf{u}}^2 - \bar{\mathcal{A}}_z(\tilde{\mathbf{B}}^1)\circ\mathfrak{d}_z\tilde{\mathbf{u}}^3 \\ &= \mathfrak{d}_y(\tilde{\mathbf{B}}^2\hat{\mathbf{u}}^1 - \tilde{\mathbf{B}}^1\hat{\mathbf{u}}^2) - \bar{\mathbf{u}}^1\circ\omega + (\tilde{\mathbf{u}}\circ\mathbf{D})\tilde{\mathbf{B}}^1 + \mathfrak{R}^{\Delta y}(\tilde{\mathbf{B}}^1, \tilde{\mathbf{B}}^2) + \mathfrak{R}^{\Delta z}(\tilde{\mathbf{B}}^1, \tilde{\mathbf{B}}^3)\end{aligned}$$

where the residual terms are

$$\mathfrak{R}^{\Delta y}(\tilde{\mathbf{B}}^1,\tilde{\mathbf{B}}^2)_{i,j,k} = \Delta y \sum_{l=-r}^{q} \left(\gamma_l^j(\tilde{\mathbf{u}}^2)\tilde{\mathbf{B}}^1_{i,j+l,k} - \gamma_l^j(\tilde{\mathbf{u}}^1)\tilde{\mathbf{B}}^2_{i,j+l,k}\right)$$

$$\mathfrak{R}^{\Delta z}(\tilde{\mathbf{B}}^1,\tilde{\mathbf{B}}^3)_{i,j,k} = \Delta z \sum_{l=-r}^{q} \left(\gamma_l^j(\tilde{\mathbf{u}}^3)\tilde{\mathbf{B}}^1_{i,j,k+l} - \gamma_l^j(\tilde{\mathbf{u}}^1)\tilde{\mathbf{B}}^3_{i,j,k+l}\right).$$

Here the γ_k^i are defined in the proof of lemma 3.1 and depend on the velocities u. Applying the same technique on the two other components we obtain

$$(\mathcal{AV}(\tilde{\mathbf{B}},\tilde{\mathbf{u}}) - (\tilde{\mathbf{u}}\circ\mathbf{D})\tilde{\mathbf{B}}) = (\mathbf{D}\times(\tilde{\mathbf{u}}\times\tilde{\mathbf{B}})) - \tilde{\mathbf{u}}\circ\hat{\omega} + \mathfrak{R}$$

where

$$\mathfrak{R} = \begin{pmatrix} \mathfrak{R}^{\Delta y}(\tilde{\mathbf{B}}^1,\tilde{\mathbf{B}}^2) + \mathfrak{R}^{\Delta z}(\tilde{\mathbf{B}}^1,\tilde{\mathbf{B}}^3) \\ \mathfrak{R}^{\Delta x}(\tilde{\mathbf{B}}^2,\tilde{\mathbf{B}}^1) + \mathfrak{R}^{\Delta z}(\tilde{\mathbf{B}}^2,\tilde{\mathbf{B}}^3) \\ \mathfrak{R}^{\Delta x}(\tilde{\mathbf{B}}^3,\tilde{\mathbf{B}}^1) + \mathfrak{R}^{\Delta y}(\tilde{\mathbf{B}}^3,\tilde{\mathbf{B}}^2) \end{pmatrix}.$$

Here $\|\mathfrak{R}\|_{\mathbf{P}} \leq C\max(\Delta x,\Delta y,\Delta z)\|\tilde{\mathbf{B}}\|_{\mathbf{P}}$. Setting these results in the discrete evolution equation an using corollary 3.3 we obtain

$$\frac{d}{dt}\hat{\omega} = -\mathbf{D}\cdot(\hat{\omega}\circ\tilde{\mathbf{u}}) + \mathbf{D}\mathfrak{R}.$$

The time evolution of the $\mathbf{P}$ norm of the divergence is

$$\frac{d}{dt}\|\bar{\omega}\|^2_{\mathbf{P}} = 2(\bar{\omega},\frac{d}{dt}\bar{\omega})_{\mathbf{P}} = -2(\bar{\omega},\mathbf{D}\cdot(\bar{\omega}\circ\tilde{\mathbf{u}}))_{\mathbf{P}} + (\bar{\omega},\mathbf{D}\mathfrak{R})_{\mathbf{P}},$$

with summation by parts and lemma 3.4 we obtain

$$\begin{aligned}\frac{d}{dt}\|\bar{\omega}\|^2_{\mathbf{P}} &= 2(\mathbf{D}\bar{\omega},\bar{\omega}\circ\tilde{\mathbf{u}})_{\mathbf{P}} + (\bar{\omega},\mathbf{D}\mathfrak{R})_{\mathbf{P}} = 2(\tilde{\mathbf{u}}\mathbf{D}\circ\bar{\omega},\bar{\omega})_{\mathbf{P}} + (\bar{\omega},\mathbf{D}\mathfrak{R})_{\mathbf{P}} \\ &= (\tilde{\mathbf{u}}\mathbf{D}\circ\bar{\omega},\bar{\omega})_{\mathbf{P}} - (\mathbf{D}\cdot(\tilde{\mathbf{u}}\circ\bar{\omega}),\bar{\omega})_{\mathbf{P}} + (\bar{\omega},\mathbf{D}\mathfrak{R})_{\mathbf{P}} \leq C\|\bar{\omega}\|^2_{\mathbf{P}} + \|\bar{\omega}\|_{\mathbf{P}}\|\mathbf{D}\mathfrak{R}\|_{\mathbf{P}} \\ &\leq C\|\bar{\omega}\|^2_{\mathbf{P}} + \frac{C}{\min(\Delta x,\Delta y,\Delta z)}\|\bar{\omega}\|_{\mathbf{P}}\|\mathfrak{R}\|_{\mathbf{P}} \leq C_1\|\bar{\omega}\|^2_{\mathbf{P}} + C_2\frac{\max(\Delta x,\Delta y,\Delta z)}{\min(\Delta x,\Delta y,\Delta z)}\|\bar{\omega}\|_{\mathbf{P}}\|\tilde{\mathbf{B}}\|_{\mathbf{P}} \end{aligned} \tag{3.17}$$

where the C's depend on u and its derivative. To obtain this result the boundary terms are neglected since $\tilde{\mathbf{B}}$ decays to 0 at infinity. We have also used that

$$(\hat{x},\tilde{\mathbf{v}}\circ\hat{y})_{\mathbf{P}} = (\tilde{\mathbf{v}}\circ\hat{x},\hat{y})_{\mathbf{P}}$$

where $\hat{x}$ and $\hat{y}$ are scalar grid function and $\tilde{\mathbf{v}}$ a vector gird function. This is the case since P is a diagonal matrix. We conclude the proof using Cauchy's inequality. □

Although the symmetric scheme (3.11) is stable in H^1, it might generate small (but bounded) divergence errors. Next, we design a scheme that preserves a discrete version of the divergence operator.

3.2. **Divergence Preserving Schemes.** The symmetric scheme does not preserve a discrete version of the divergence constraint as it discretizes the symmetric version (2.2) of the Hall induction equations. We have to discretize the non-symmetric standard version (1.11) of the Hall induction equations in order to design a divergence preserving scheme. Such a scheme for is

$$\begin{aligned}\frac{d}{dt}\left(\tilde{\mathbf{B}}_{i,j,k} + \left(\frac{\delta_e}{L_0}\right)^2\frac{1}{\rho}(\mathbf{D}\times\mathbf{D}\times\tilde{\mathbf{B}})_{i,j,k}\right) &= \mathbf{D}\times(\tilde{\mathbf{u}}\times\tilde{\mathbf{B}}_{i,j,k}) - \eta(\mathbf{D}\times(\mathbf{D}\times\tilde{\mathbf{B}}_{i,j,k})) \\ - \left(\frac{\delta_e}{L_0}\right)^2\frac{1}{\delta}\mathbf{D}\times((\tilde{\mathbf{u}}_{i,j,k}\cdot\mathbf{D})(\mathbf{D}\times\tilde{\mathbf{B}}_{i,j,k})) &- \frac{\delta_i}{L_0}\frac{1}{\delta}\mathbf{D}\times((\mathbf{D}\times\tilde{\mathbf{B}}_{i,j,k})\times\tilde{\mathbf{B}}_{i,j,k}).\end{aligned} \tag{3.18}$$

The application of corollary 3.3 shows that the above scheme clearly satisfies the divergence constraint:

$$\frac{d}{dt}\mathbf{D}\cdot\tilde{\mathbf{B}} = 0. \tag{3.19}$$

The proof for the energy stability of this scheme is more complex since the equation is not symmetric. We introduce the following one-sided operators:

$$D_x^s w_i = \frac{w_{i+s} - w_i}{s\Delta x}. \tag{3.20}$$

The operators D_y^s and D_z^s are defined analogously.

Lemma 3.6. *For two grid functions u and w , the following identity holds,*

$$D_x(u \circ w) = u \circ D_x w + \hat{A}_x((D_x^s u), w), \tag{3.21}$$

with $\hat{A}_x((D_x^s u), w)_i = \sum_k k\beta_k (D_x^k u_i) w_{i+k}$ is an average over discrete one sided derivative of u multiplied with w.

Proof. We compute the difference

$$\begin{aligned} D_x(u \circ w)_i - u \circ D_x w &= \frac{1}{\Delta x}\sum_k \beta_k u_{i+k} w_{i+k} - u_i \frac{1}{\Delta x}\sum_k \beta_k w_{i+k} \\ &= \frac{1}{\Delta x}\sum_k \beta_k k \frac{u_{i+k} - u_i}{k\Delta x} w_{i+k}, \end{aligned}$$

noting that it takes the form of the desired average. □

The energy bound for the divergence preserving scheme is given below:

Theorem 3.3. *Let $\tilde{\mathbf{u}}_{i,j,k} = \mathbf{u}(x_i, y_j, z_k)$ be the point evaluation of a function $u \in C^2$ and let the solutions of (3.18) with an initial data with $\mathbf{D} \cdot \tilde{\mathbf{B}}_0 = 0$. If the approximate solution decays to zero at infinity, then the following estimates hold*

$$\frac{d}{dt}\left(\|\tilde{\mathbf{B}}\|_{\mathbf{P}}^2 + \left(\frac{\delta_e}{L_0}\right)^2 \frac{1}{\rho}\|\mathbf{D} \times \tilde{\mathbf{B}}\|_{\mathbf{P}}^2 \right) \leq C \left(\|\tilde{\mathbf{B}}\|_{\mathbf{P}}^2 + \left(\frac{\delta_e}{L_0}\right)^2 \frac{1}{\rho}\|\mathbf{D} \times \tilde{\mathbf{B}}\|_{\mathbf{P}}^2 \right) \tag{3.22}$$

with C a constant that depends on $\mathbf{u}$ and its derivative only.

Proof. To prove the energy estimate, we have to symmetrize the advection terms in the scheme. This is possible since the method preserve divergence; in this case we can subtract form (3.18) $\tilde{\mathbf{v}}(\mathbf{D} \cdot \tilde{\mathbf{B}}) = 0$.
Using lemma (3.6), we cam reformulate the discrete advection part

$$\mathbf{D} \times (\tilde{\mathbf{u}} \times \tilde{\mathbf{B}}) - \tilde{\mathbf{v}}(\mathbf{D} \cdot \tilde{\mathbf{B}}) = -(\tilde{\mathbf{u}} \cdot \mathbf{D})\tilde{\mathbf{B}} + \mathcal{R}(\tilde{\mathbf{B}}, \tilde{\mathbf{u}}),$$

with

$$\mathcal{R}(\tilde{\mathbf{B}}, \tilde{\mathbf{u}})_{i,j,k} = \begin{pmatrix} \mathcal{A}_y[(\mathfrak{d}_y^s(\hat{u}_1)\hat{B}_2)_{i,j,k} - (\mathfrak{d}_y^s(\hat{u}_2)\hat{B}_1)_{i,j,k}] + \mathcal{A}_z[(\mathfrak{d}_z^s(\hat{u}_1)\hat{B}_3)_{i,j,k} - (\mathfrak{d}_z^s(\hat{u}_3)\hat{B}_1)_{i,j,k}] \\ \mathcal{A}_x[(\mathfrak{d}_y^s(\hat{u}_2)\hat{B}_1)_{i,j,k} - (\mathfrak{d}_x^s(\hat{u}_1)\hat{B}_2)_{i,j,k}] + \mathcal{A}_z[(\mathfrak{d}_z^s(\hat{u}_2)\hat{B}_3)_{i,j,k} - (\mathfrak{d}_z^s(\hat{u}_3)\hat{B}_2)_{i,j,k}] \\ \mathcal{A}_x[(\mathfrak{d}_x^s(\hat{u}_3)\hat{B}_1)_{i,j,k} - (\mathfrak{d}_x^s(\hat{u}_1)\hat{B}_3)_{i,j,k}] + \mathcal{A}_y[(\mathfrak{d}_y^s(\hat{u}_3)\hat{B}_2)_{i,j,k} - (\mathfrak{d}_y^s(\hat{u}_2)\hat{B}_3)_{i,j,k}] \end{pmatrix}.$$

The resulting scheme is

$$\begin{aligned} \frac{d}{dt}\left(\tilde{\mathbf{B}}_{i,j,k} + \left(\frac{\delta_e}{L_0}\right)^2 \frac{1}{\rho}(\mathbf{D} \times \mathbf{D} \times \tilde{\mathbf{B}})_{i,j,k} \right) &= -(\tilde{\mathbf{u}} \cdot D)\tilde{\mathbf{B}} + \mathcal{R}(\tilde{\mathbf{u}}, \tilde{\mathbf{B}}) - \eta(\mathbf{D} \times (\mathbf{D} \times \tilde{\mathbf{B}}_{i,j,k})) \\ &- \left(\frac{\delta_e}{L_0}\right)^2 \frac{1}{\delta}\mathbf{D} \times ((\tilde{\mathbf{u}}_{i,j,k} \cdot \mathbf{D})(\mathbf{D} \times \tilde{\mathbf{B}}_{i,j,k})) - \frac{\delta_i}{L_0}\frac{1}{\delta}\mathbf{D} \times ((\mathbf{D} \times \tilde{\mathbf{B}}_{i,j,k}) \times \tilde{\mathbf{B}}_{i,j,k}) \end{aligned}$$

We see that this is very similar to result obtained for the symmetric case. The only difference is that, instead the average term $(\tilde{\mathbf{B}}, \mathcal{AV}(\tilde{\mathbf{B}}, \mathbf{u}))_{\mathbf{P}}$ we have a residual term $(\tilde{\mathbf{B}}, \mathcal{R}(\tilde{\mathbf{B}}, \mathbf{u}))_{\mathbf{P}}$. Then showing that the residual term is bounded

$$(\tilde{\mathbf{B}}, \mathcal{R}(\tilde{\mathbf{B}}, \mathbf{u}))_{\mathbf{P}} \leq C\|\tilde{\mathbf{B}}\|_{\mathbf{P}}^2$$

will conclude the proof. We can follow the same procedure we used in the proof of lemma 3.5 to bound the advection term. □

The proof follows the theory presented in [9] where a generalized finite volume scheme that preserve discrete divergence is presented. The method presented there is more general in its formulation, and includes a large class of already known divergence preserving methods.

3.3. **Time Stepping.** Both the semi-discrete symmetric scheme and divergence preserving schemes can be written as

$$\frac{d}{dt}\left(\hat{\mathbf{B}} + \alpha \mathbf{D}\times\mathbf{D}\times\hat{\mathbf{B}}\right) = \mathcal{RHS}(\hat{\mathbf{B}},\hat{\mathbf{u}}), \tag{3.23}$$

with $\alpha = \left(\frac{\delta_e}{L_0}\right)^2 \frac{1}{\rho}$ and the function $\mathcal{RHS}$ will depend on the scheme.

We use a standard Runge Kutta method to update the solution in time. Even though we use explicit RK methods, we have to solve linear equations (corresponding to the lhs of the above scheme) at each time step. As an example, we consider a second order SSP method ([4]):

$$\begin{aligned}
\hat{\mathbf{B}}^{\star} &= \hat{\mathbf{B}}^n + \Delta t A^{-1}\mathcal{RHS}(\hat{\mathbf{B}}^n,\hat{\mathbf{u}}),\\
\hat{\mathbf{B}}^{\star\star} &= \hat{\mathbf{B}}^{\star} + \Delta t A^{-1}\mathcal{RHS}(\hat{\mathbf{B}}^{\star},\hat{\mathbf{u}},)\\
\hat{\mathbf{B}}^{n+1} &= \frac{\hat{\mathbf{B}}^n + \hat{\mathbf{B}}^{\star\star}}{2}.
\end{aligned} \tag{3.24}$$

Here, $A = I + \alpha F$, F is the matrix representation of $\mathbf{D}\times\mathbf{D}$ and I is the identity matrix. In this paper, we are using a direct solver. However, the matrices F and A are of size $3\times N_x\times N_y\times N_z$, and not well conditioned for high-resolution meshes. The design of an efficient preconditioner for the matrix A is a subject of ongoing research.

4. Numerical Experiments

For simplicity, we consider the Hall induction equations in two space dimensions and present numerical experiments comparing different schemes proposed above. In two space dimensions, the symmetric version (2.2) reads as

$$\begin{aligned}
\frac{\partial}{\partial t}\left[\hat{\mathbf{B}} + \left(\frac{\delta_e}{L_0}\right)^2\frac{1}{\rho}\widehat{\nabla}\times\widehat{\nabla}\times\hat{\mathbf{B}}\right] &= \hat{C_1}\hat{\mathbf{B}} - (\hat{\mathbf{u}}\cdot\nabla)\hat{\mathbf{B}} - \eta\widehat{\nabla}\times\widehat{\nabla}\times\hat{\mathbf{B}} - \left(\frac{\delta_e}{L_0}\right)^2\frac{1}{\rho}\widehat{\nabla}\times((\hat{\mathbf{u}}\cdot\nabla)(\widehat{\nabla}\times\hat{\mathbf{B}}))\\
&\quad - \frac{\delta_i}{L_0}\frac{1}{\rho}\widehat{\nabla}\times(\hat{\mathbf{B}}\cdot\nabla B_3),
\end{aligned} \tag{4.1a}$$

$$\begin{aligned}
\frac{\partial}{\partial t}\left[B_3 - \left(\frac{\delta_e}{L_0}\right)^2\frac{1}{\rho}\Delta B_3\right] &= \mathbf{C}_2\mathbf{B} - \hat{\mathbf{u}}\nabla B_3 + \eta\Delta B_3 + \left(\frac{\delta_e}{L_0}\right)^2\frac{1}{\rho}\nabla\cdot((\hat{\mathbf{u}}\cdot\nabla)\nabla B_3)\\
&\quad - \frac{\delta_i}{L_0}\frac{1}{\rho}\nabla\cdot(\hat{\mathbf{B}}\cdot(\widehat{\nabla}\times\hat{\mathbf{B}})).
\end{aligned} \tag{4.1b}$$

Here, $\hat{\mathbf{B}} = (B_1, B_2)^\top$ and $\hat{\mathbf{u}} = (u_1, u_2)^\top$. We have also introduced a compact "curl" operator $\widehat{\nabla}\times$ in two dimensions:

$$\widehat{\nabla}\times\begin{pmatrix} v_1\\ v_2\end{pmatrix} := \frac{\partial v_2}{\partial x} - \frac{\partial v_1}{\partial y} \tag{4.2a}$$

$$\widehat{\nabla}\times\psi := \begin{pmatrix} \frac{\partial\psi}{\partial y}\\ -\frac{\partial\psi}{\partial x}\end{pmatrix}, \tag{4.2b}$$

where $\hat{\mathbf{v}}:\mathbb{R}^3\to\mathbb{R}^2$ and $\psi:\mathbb{R}^3\to\mathbb{R}$. We consider the following numerical experiments:

4.1. **Pure advection.** First, we test the proposed numerical schemes for the magnetic induction equations without Hall, electron inertia and resistivity terms. We take the velocity field

$$\mathbf{u} = (-y, x)^\top$$

in the following. Then, (4.1) with $\eta = \delta_i = \delta_e = 0$ has an exact solution (see [2]) given by

$$\hat{\mathbf{B}}(x, y, y) = R(t)\hat{\mathbf{B}}_0(R(-t)(x.y)), \tag{4.3}$$

with $R(t)$ a rotation matrix with angle t.

The initial data is

$$\hat{\mathbf{B}}_0(x, y) = 4 \begin{pmatrix} -y \\ x - \frac{1}{2} \end{pmatrix} e^{-20((x-1/2)^2+y^2)} \tag{4.4}$$

in the computational domain $\Omega = [-2.5, 2.5] \times [-2.5, 2.5]$. We consider Neumann type non-reflecting boundary conditions. The exact solution represents the rotation of the initial hump around the domain with the hump completing one rotation in the period $T = 2\pi$.

We will test the following four schemes: the second- and fourth-order versions of the symmetric scheme (3.11) with difference operators given in appendix A, second- and fourth-order version of the divergence preserving scheme (3.18). The convergence plots in L^2 are shown in figure 1.

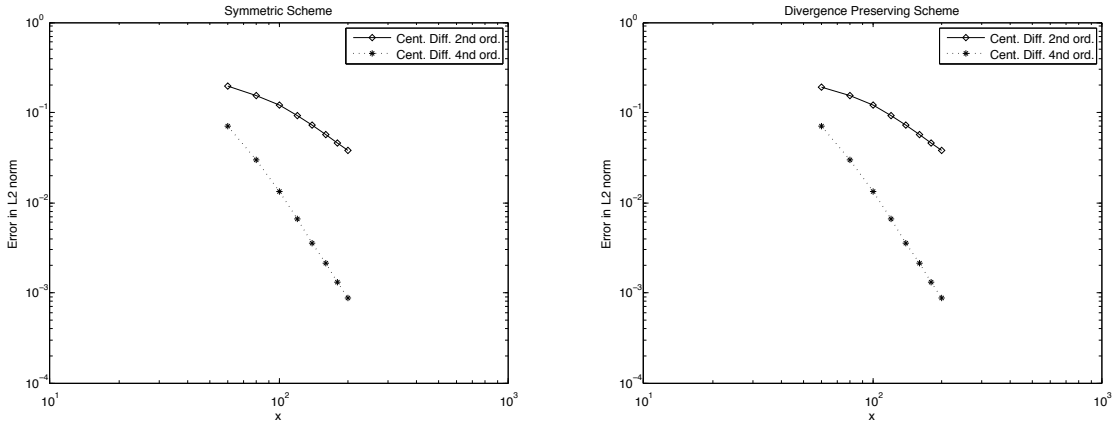

(a) Symmetric schemes (b) Divergence preserving schemes

FIGURE 1. Convergence plots for the advection problem for the different schemes analyzed.

For time integration we have used a second order SSP and a standard third order Runge-Kutta method. The results are obtained using different mesh sizes, form 80 to 200 points. The experimental convergence orders are shown in Table 1 and demonstrate that the expected orders of accuracy are obtained in practice.

	2nd ord	4 ord
Preserving	1.89	3.98
Symmetric	1.89	3.98

TABLE 1. Convergence rates for the advection Problem.

4.2. **Forced Solutions.** In order to test the convergence rates for various schemes for full Hall induction equations, we add a forcing term such that the rotating hump (4.3) remains a solution of the forced equations. The Hall induction equations with the forcing term are

$$\begin{aligned}\frac{\partial}{\partial t}\left[\hat{\mathbf{B}} + \left(\frac{\delta_e}{L_0}\right)^2 \frac{1}{\rho}\widehat{\nabla}\times\widehat{\nabla}\times\hat{\mathbf{B}}\right] &= \hat{C_1}\hat{\mathbf{B}} - (\hat{\mathbf{u}}\cdot\nabla)\hat{\mathbf{B}} - \eta\widehat{\nabla}\times\widehat{\nabla}\times\hat{\mathbf{B}} - \left(\frac{\delta_e}{L_0}\right)^2 \frac{1}{\rho}\widehat{\nabla}\times((\hat{\mathbf{u}}\cdot\nabla)(\widehat{\nabla}\times\hat{\mathbf{B}})) \\ &\quad - \frac{\delta_i}{L_0}\frac{1}{\rho}\widehat{\nabla}\times(\hat{\mathbf{B}}\cdot\nabla B_3) + \hat{\mathbf{S}}(x,y,t), \\ \frac{\partial}{\partial t}\left[B_3 - \left(\frac{\delta_e}{L_0}\right)^2 \frac{1}{\rho}\Delta B_3\right] &= \mathbf{C}_2\mathbf{B} - \hat{\mathbf{u}}\nabla B_3 + \eta\Delta B_3 + \left(\frac{\delta_e}{L_0}\right)^2 \frac{1}{\rho}\nabla\cdot((\hat{\mathbf{u}}\cdot\nabla)\nabla B_3) \\ &\quad - \frac{\delta_i}{L_0}\frac{1}{\rho}\nabla\cdot(\hat{\mathbf{B}}\cdot(\widehat{\nabla}\times\hat{\mathbf{B}})) + S^3(x,y,t).\end{aligned}$$

We forcing term $\hat{\mathbf{S}}$ is

$$\begin{aligned}\hat{\mathbf{S}}(x,y,t) &= 160\,P(x,y,t)\,\eta\,e^{-20((x\cos(t)+y\sin(t)-1/2)^2+(y\cos(t)-x\sin(t))^2}\begin{pmatrix}\sin(t)-2y\\ 2x-\cos(t)\end{pmatrix}, \\ S^3(x,y,t) &= 0.\end{aligned}$$

Here $P(x,y,t) = 20x\cos(t) + 20y\sin(t) - 20x^2 - 20y^2 - 3$.

The convergence results for four different schemes are presented in figure. The obtained orders of convergence are shown in Table 2. Again, the expected orders of convergence are obtained.

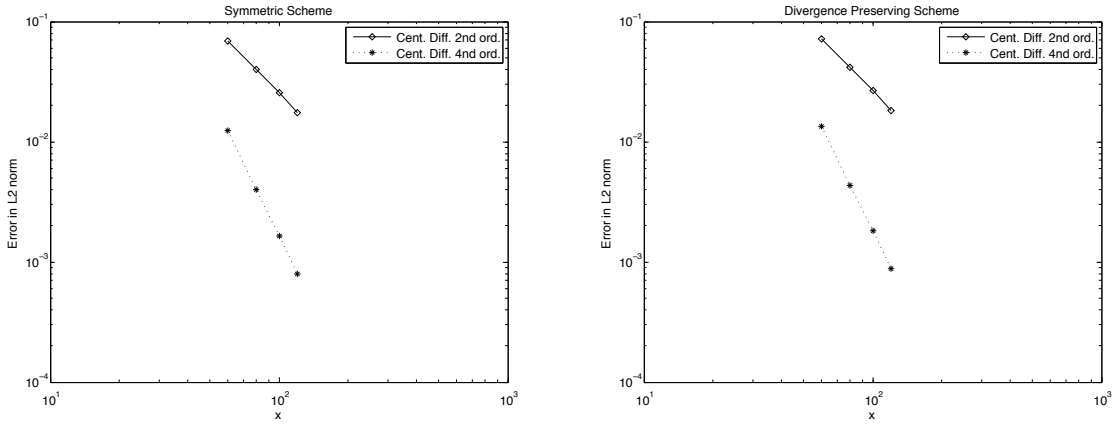

(a) Symmetric schemes (b) Divergence preserving schemes

FIGURE 2. Convergence plots for the Forced Problem with $\eta = 0.01$,$\delta_i = 0.1$ and $\delta_e = 4.5\times10^{-2}$

	2nd ord	4 ord
Preserving	2.05	3.97
Symmetric	2.05	3.98

TABLE 2. Convergence rates for the Forced Problem with $\eta = 0.01$,$\delta_i = 0.1$ and $\delta_e = 4.5\times10^{-2}$

4.3. **Unforced solutions.** In the final numerical experiment, we test the full Hall induction equations (without any forcing) for the rotating hump problem. We set $\eta = 0.01$, $\delta_i = 0.1$ and $\delta_e = 4.5 \times 10^{-2}$ and compute the solutions on a mesh 160×160 points. We compare the results with those obtained for the pure advection of the hump. The results are shown in figure 3 and demonstrate the robustness of the second-order symmetric scheme. Similar results were obtained with the divergence preserving scheme. The results show that the addition of resistivity, electron inertia and Hall effect leads to diffusion of the original hump and the creation of a non-zero B_3 component even if the initial B_3 is set to zero.

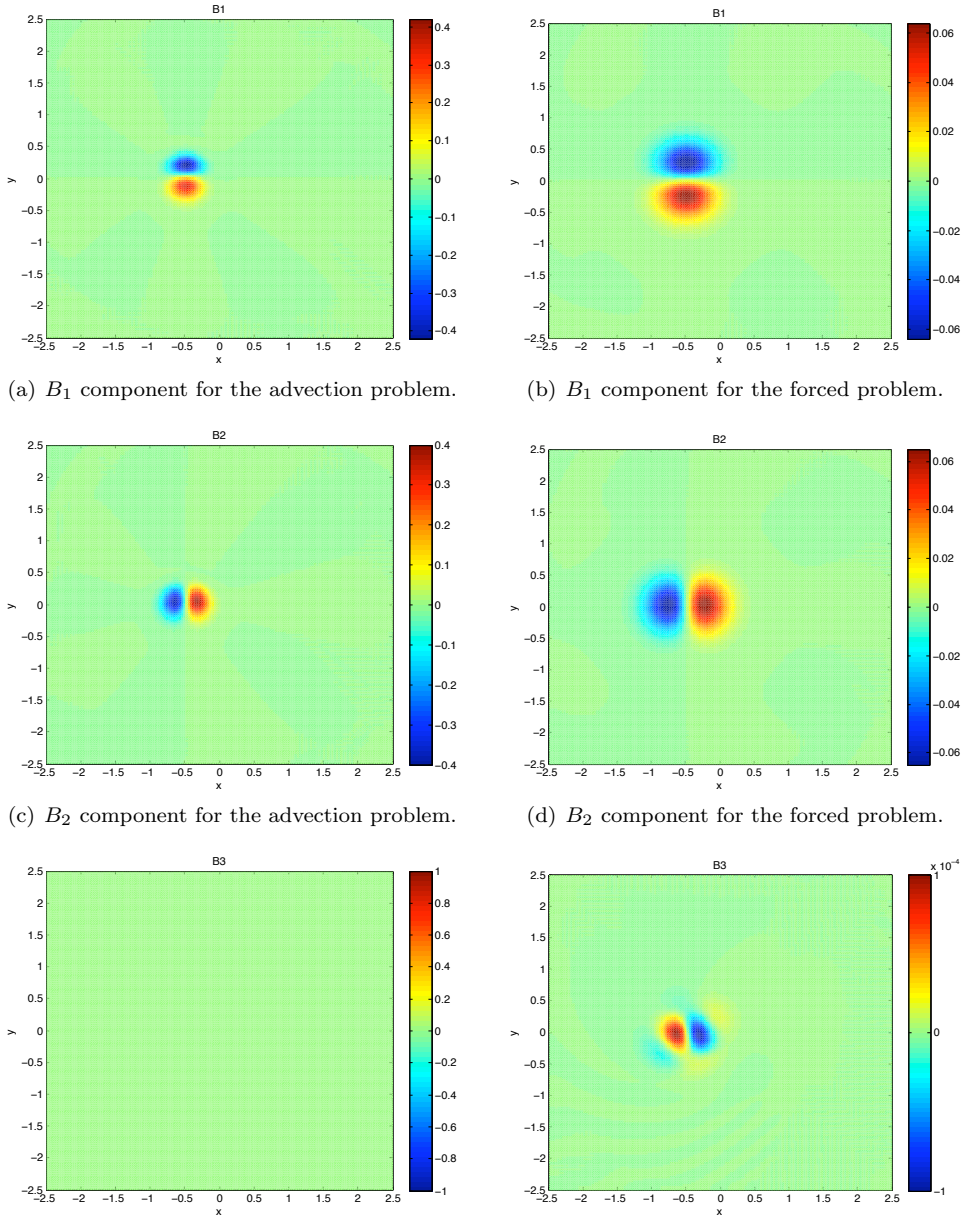

(a) B_1 component for the advection problem.

(b) B_1 component for the forced problem.

(c) B_2 component for the advection problem.

(d) B_2 component for the forced problem.

(e) B_3 component for the advection problem.

(f) B_3 component for the forced problem.

FIGURE 3. On the right plots for solution with $\eta = 0.01$,$\delta_i = 0.1$ and $\delta_e = 4.5 \times 10^{-2}$ after $T = \pi$ and on the left the advected solution after the same time.

We conclude by tabulating the discrete divergence generated by the schemes for this problem in Table 3. As expected, the divergence preserving scheme *preserves* divergence to machine precision. On the other hand, the symmetric scheme does generate some spurious divergence.

	Symmetric	Preserving
25	$4.6e-2$	$6.4e{-}17$
50	$2.4e-5$	$8.6e-17$
75	$6.2e-7$	$9.1e-17$
100	$2.5e-7$	$1.1e-16$
125	$1.4e-7$	$1.2e-16$

TABLE 3. Discrete divergence for the unforced problem.

The divergence errors converge quite rapidly to zero as the mesh is refined. Furthermore, there was no noticeable difference in the quality of the results for the primary solution variables between the symmetric and divergence preserving schemes.

5. Conclusion

We consider the Hall induction equation, a sub-model for the Hall MHD equations, in this paper. An energy estimate is derived for the equations and numerical schemes that satisfy a discrete version of this estimate are presented. A special class of numerical schemes also satisfy the divergence constraint. The proposed schemes are tested on a set of numerical examples and are demonstrated to be robust. The extension of the schemes to the full Hall MHD equations is the subject of forthcoming papers.

Appendix A. Finite Difference Operators

The different operators used in our numerical experiment, are based on one dimensional operators coupled together with Kronecker product. The one dimensional operators are given for $q = x, y, z$ in matrix form:

- Second order central difference

$$D_q^{(2)} = P_q^{-1}Q = \frac{1}{2\Delta q}\begin{pmatrix} -2 & 2 & & & \\ -1 & 0 & 1 & & \\ & \ddots & \ddots & \ddots & \\ & & -1 & 0 & 1 \\ & & & -2 & 2 \end{pmatrix}, \qquad P_q = \Delta q \begin{pmatrix} \frac{1}{2} & & & & \\ & 1 & & & \\ & & \ddots & & \\ & & & 1 & \\ & & & & \frac{1}{2} \end{pmatrix}.$$

- Fourth order central difference

$$D_q^{(4)} = P_q^{-1}Q = \frac{1}{\Delta q}\begin{pmatrix} -1 & 1 & & & & & \\ -\frac{1}{2} & 0 & \frac{1}{2} & & & & \\ \frac{1}{12} & -\frac{2}{3} & 0 & \frac{2}{3} & -\frac{1}{12} & & \\ & \ddots & \ddots & \ddots & \ddots & \ddots & \\ & & \frac{1}{12} & -\frac{2}{3} & 0 & \frac{2}{3} & -\frac{1}{12} \\ & & & & -\frac{1}{2} & 0 & \frac{1}{2} \\ & & & & & -1 & 1 \end{pmatrix}, \qquad P_q = \Delta q \begin{pmatrix} \frac{1}{2} & & & & & & \\ & 1 & & & & & \\ & & \ddots & & & & \\ & & & 1 & & & \\ & & & & \ddots & & \\ & & & & & 1 & \\ & & & & & & \frac{1}{2} \end{pmatrix}.$$

Combining this operators we obtain the two spatial discretisation used in the numerical experiments.
We give the discrete derivative for the x direction, the ones for the other spatial directions are defined analogously.
Standard second and fourth order operator are

$$\mathfrak{d}_x = D_x^{(k)} \otimes I_y \otimes I_z \quad k = 2, 4$$

where I_q are the identity matrices.

References

[1] D. Biskamp, Nonlinear Magnetohydrodynamics *Cambridge University Press, New York*, 1993.

[2] F.G. Fuchs, K. Karlsen, S. Mishra and N.H. Risebro. Stable upwind schemes for the magnetic induction equation. *Mathematical Modeling and Numerical Analysis,***43(5)**, 825- 852, 2009.

[3] F.G. Fuchs, A.D. McMurry, S. Mishra, N.H. Risebro and K.Waagan Simulating waves in the upper solar atmosphere with SURYA: a well-balanced high-order finite volume code. *Astrophysical Jl.,* To appear.

[4] S. Gottlieb, C-W.Shu and E. Tadmor, Strong stability-preserving high-order time discretisation method, *SIAM Review*, **43**, 89-112, 2001.

[5] U. Koley, S. Mishra, N.H. Risebro and M. Svärd, Higher order finite difference schemes for the magnetic induction equations with resistivity. *IMA Jl. Num. Anal.,*, To appear.

[6] U. Koley, S. Mishra, N.H. Risebro and M. Svärd, Higher order finite difference schemes for the magnetic induction equations. *BIT Numerical Mathematics*, **49,2**, 375-395, 2009.

[7] Z.W. Ma and A. Bhattacharjee, Hall magnetohydrodynamic reconnection: The Geospace Environment challenge. *Journal of Geophysical Research,* **106**, 3773 -3782, 2001.

[8] S. Mishra and M. Svärd, On stability of numerical scheme via frozen coefficients and magnetic induction equations, *BIT Numerical Mathematics*, **50,1**, 85-108, 2010.

[9] S.Mishra and E.Tadmor, Constraint preserving schemes using potential-based fluxes. I. Multidimensional transport equations, *Communication in Computational Physics,*,**9,3**,688-710, 2010.

[10] X. Qian, J. Balbás, A. Bhattacharjee and H. Yang A Numerical Study of Magentic Reconnection: A Central Scheme for Hall, *Hyperbolic Partial Differential Equations, Theory, Numerics and Applications*, Proceedings of the 12th. international conference held at the University of Maryland.

[11] M. Svrd and J. Nordstrm On the order of accuracy for difference approximations of initial-boundary value problems, *Journal of Computational Physics vol,***218**, 333-352,2006.

[12] M. Torrilhon and M. Fey Constraint-preserving upwind methods for multidimensional advection equations. *SIAM Journal of Numerical Analysis,***42,4**,1694-1728,2004.

[13] G. Toth, Y. J. Ma and T. I. Gombosi Hall Magnetohydrodynamics on Block Adaptive Grids. *Journal of Computational Physics,***227**,6967-6984,2008.

(Paolo Corti)
Seminar For Applied Mathematics (SAM)
ETH Zentrum
Rämistrasse 101
8092 Zürich
E-mail address: paolo.corti@sam.math.ethz.ch

(Siddhartha Mishra)
Seminar For Applied Mathematics (SAM)
ETH Zentrum
Rämistrasse 101
8092 Zürich
E-mail address: siddhartha.mishra@sam.math.ethz.ch

Research Reports

No.	Authors/Title
11-23	*P. Corti and S. Mishra* Stable finite difference schemes for the magnetic induction equation with Hall effect
11-22	*H. Kumar and S. Mishra* Entropy stable numerical schemes for two-fluid MHD equations
11-21	*H. Heumann, R. Hiptmair, K. Li and J. Xu* Semi-Lagrangian methods for advection of differential forms
11-20	*A. Moiola* Plane wave approximation in linear elasticity
11-19	*C.J. Gittelson* Uniformly convergent adaptive methods for parametric operator equations
11-18	*E. Kokiopoulou, D. Kressner, M. Zervos and N. Paragios* Optimal similarity registration of volumetric images
11-17	*D. Marazzina, O. Reichmann and Ch. Schwab* *hp*-DGFEM for Kolmogorov-Fokker-Planck equations of multivariate Lévy processes
11-16	*Ch. Schwab and A.M. Stuart* Sparse deterministic approximation of Bayesian inverse problems
11-15	*A. Barth and A. Lang* Almost sure convergence of a Galerkin–Milstein approximation for stochastic partial differential equations
11-14	*X. Claeys* A single trace integral formulation of the second kind for acoustic scattering
11-13	*W.-J. Beyn, C. Effenberger and D. Kressner* Continuation of eigenvalues and invariant pairs for parameterized nonlinear eigenvalue problems
11-12	*C.J. Gittelson* Adaptive stochastic Galerkin methods: beyond the elliptic case
11-11	*C.J. Gittelson* An adaptive stochastic Galerkin method